



INVESTIGATION OF PHYSICAL AND CHEMICAL PROPERTIES OF 2-[(2-HYDROXY-4-NITROPHENYL)AMINOMETHYLENE]-CYCLOHEXA-3,5-DIEN-1(2H)-ONE BY DFT METHOD

*Cem Cüneyt ERSANLI¹, Başak KOŞAR²

¹Sinop University, Faculty of Arts and Sciences, Department of Physics, Sinop, ccersanli@sinop.edu.tr

²Sinop University, Faculty of Education, Department of Science Education, Sinop, bkosar@sinop.edu.tr

ABSTRACT

This work presents the characterization on the tautomeric forms of 2-[(2-hydroxy-4-nitrophenyl)aminomethylene]cyclohexa-3,5-dien-1(2H)-one, (I), quantum chemical calculations. The tautomeric forms of I in gas-phase and various solvents have been defined at the B3LYP/6-311+G(d,p) level of density functional theory (DFT). DFT calculations of non-linear optical (NLO) properties, natural bond orbital (NBO) analysis, frontier molecular orbitals (FMOs), molecular electrostatic potential (MEP) and thermodynamic properties with temperature ranging from 100 K to 300 K have been defined at the same level of theory. In addition, Mulliken population analysis of I have been performed at B3LYP/6-31(d) level of DFT.

Keywords: Schiff base, tautomeric form, DFT, MEP.

YFT METODUYLA 2-[(2-HİDROKSİ-4-NİTROFENİL)AMİNOMETİLEN]SİKLOHEKSA-3,5-DİYEN-1(2H)-ON'UN FİZİKSEL VE KİMYASAL ÖZELLİKLERİNİN ARAŞTIRILMASI

ÖZET

Bu çalışmada tautomerik formlardaki 2-[(2-hidroksi-4-nitrofenil)amino metilen]siklohekza-3,5-diyen-1(2H)-on (I)'un kuantum kimyasal hesaplamalar ile karakterizasyonu sunulmaktadır. Gaz fazında ve çeşitli çözücü fazlarında bileşiğin tautomerik formları B3LYP/6-311+G(d,p) teori seviyesinde yoğunluk fonksiyonel teori (YFT) ile belirlenmiştir. Doğrusal-olmayan optik özellikleri, doğal bağ orbital analizi, sınır moleküler orbitalleri, moleküler elektrostatik potansiyel (MEP) ve 100 K ile 300 K arasındaki sıcaklık aralığında termodinamik özellikleri yoğunluk fonksiyonel teori ile aynı baz setinde hesaplanmıştır. Bunlara ek olarak, bileşiğin Mulliken populasyon analizi B3LYP/6-31(d) teori seviyesinde YFT hesaplamaları ile gerçekleştirilmiştir.

Anahtar Kelimeler: Schiff bazı, tautomerik form, YFT, MEP.

1. INTRODUCTION

The Schiff base compounds can be classified according to their photochromic and thermochromic characteristics [1]. *o*-Hydroxy Schiff bases derived from the reaction of *o*-hydroxy aldehydes with aniline have been examined extensively [2-3]. Some Schiff bases derived from salicylaldehyde have attracted the interest of chemists and physicists because they show thermochromism and photochromism in the solid state by H-atom transfer from the hydroxy O atom to the N atom [4]. It has been proposed that molecules showing thermochromism are planar, while those showing photochromism are non-planar [5]. Because of its intramolecular hydrogen bonding, depending on the position of proton in the hydrogen bond *o*-hydroxy salicylidene Schiff bases exhibit two tautomeric forms, the keto-amine (or quinoid) and enol-imine (or benzenoid) both in solution and in crystalline state.

By way of increasing development of computational chemistry in the past decade, the research of theoretical modeling of drug design, functional material design, *etc.*, has become much more mature than ever. Many important chemical and physical properties of biological and chemical systems can be predicted from the first principles by various computational techniques. In conjunction with the development of technology, DFT has been favorite one due to its great accuracy in reproducing the experimental values of in molecule geometry, atomic charges, dipole moments, *etc.* [6]. In previous publication, the X-ray crystallography of **I** were studied [7]. In spite of its importance, mentioned above, there is no any theoretical calculation on **I** has been published yet. The purpose of this study is to investigate the energetic and structural properties of **I**, using DFT calculations. At the same time in this work, second-order non-linear optical, NBO, FMOs, MEP, thermodynamic properties and Mulliken population analysis of **I** were investigated.

2. COMPUTATIONAL ASPECTS

In computational procedure, complete geometrical optimizations of the investigated molecule is performed using DFT with the Becke's three parameters exchange functional with the Lee-Yang-Parr nonlocal correlation functional B3LYP [6,8] with 6-311+G(d,p) basis set. Firstly, the calculations were started with the crystallographically obtained geometrical data for the keto-amine form of **I**. Total molecular energy and dipole moment (μ) were obtained from the optimization output. In addition, a theoretical enol-imine form of **I** was drawn and optimized with the similar optimization circumstances. All calculations were performed by using the Gaussian03W software package [9] and GaussView program [10] package, running under Windows 7 Professional on a Intel Core™2 Duo CPU/2.93 GHz processor was used for the molecular visualization of calculated structures on a personal computer. Secondly, in order to investigate the solvent effect on the calculated geometric parameters, we used four different kinds solvent (chloroform, acetone, ethanol, and DMSO) at the B3LYP/6-311+G(d,p) level using Polarizable Continuum Model (PCM) method [11-12]. Thirdly, to investigate the tautomeric stability, some properties such as total energy, the highest occupied molecular orbital (HOMO) and the lowest unoccupied molecular orbitals (LUMO) energies, μ , the global hardness (η), electronegativity (χ) and softness (σ) for keto-amine and the enol-imine forms of **I** were obtained at B3LYP/6-311+G(d,p) level in gas-phase. These properties were also examined for **I** in solvent media using the PCM method. Fourthly, in order to show NLO activity and reactive sites of the molecule, the linear polarizability (α) and the first hyperpolarizability (β) were obtained by the molecular polarizabilities using polar=ENONLY

input to Gaussian 03W with the same level of theory. Fifthly, the natural atomic charges are calculated using NBO calculations as implemented in the Gaussian 03 package [13] at B3LYP/6-311+G(d,p) method from gas-phase. Sixthly, FMOs, MEP and thermodynamic functions were obtained at the same method. Finally, the other molecular properties like Mulliken population analysis of I were investigated by theoretical calculation results at B3LYP/6-31G(d) level in gas-phase and three different kinds solvent.

3. RESULTS AND DISCUSSION

3.1. Tautomeric Forms of I in Gas and Solvent-Phases

2-[(2-Hydroxy-4-nitrophenyl)amino methylene]cyclohexa-3,5-dien-1(2H)-one crystallize in monoclinic space group $P2_1/c$, the crystal structure parameters of I are $a = 11.9528(13) \text{ \AA}$, $b = 8.0910(5) \text{ \AA}$, $c = 12.4205(14) \text{ \AA}$ and $\beta = 108.268(9)^\circ$, and molecule adopts the keto-amine form rather than the enol-imine form [7]. The selected optimized parameters in gas-phase for keto-amine and enol-imine forms and in different solvents for keto-amine form are listed in Table 1. As shown in Table 1, most of the calculated bond lengths and the bond angles are slightly different from the experimental ones. The difference between experimental and calculated values of bond lengths is not more than 0.02 \AA except the bonds N1-C7 and C1-O1 differ by lengths 0.032 and 0.044 \AA in the gas-phase, $0.028/0.022/0.021/0.021 \text{ \AA}$ and $0.035/0.030/0.030/0.031 \text{ \AA}$ in the chloroform/acetone/ethanol/DMSO, respectively, for the keto-amine form of title molecule. In enol-imine form of title molecule, the difference between experimental and calculated values of bond lengths is not more than 0.02 \AA except the bonds C6-C7 and C1-O1 differ by lengths 0.042 and 0.041 \AA . The bond angles differ by not more than 1° except the angles, O3-N2-O4, O4-N2-C11 and C8-C9-O2 which differ by 1.54 , 1.06 and 1.05° in the gas-phase and solvents for the keto-amine form. In enol-imine form, the difference between experimental and calculated values of bond angles is not more than 1° except the angles, O3-N2-O4, O4-N2-C11, C7N1-C8, C2-C1-O1 and C10-C9-O2 differ by angles 1.51 , 1.07 , 6.43 , 3.27 and 1.21° . These differences are because the theoretical calculations are performed for gas-phase and solvents while experimental results belong to solid phase. In the solid state the experimental results are regarded to molecular packing, but in the gas-phase and solvents the isolated molecules are considered in the theoretical calculations.

Table 1. Selected bond lengths, bond and torsion angles for **I**.

Parameters	Experimental	DFT-B3LYP/6-311+G(d,p)					Enol-imine form Gas-Phase ($\epsilon=1$)
	X-ray [7]	Keto-amine form					
		Gas-Phase ($\epsilon=1$)	Chloroform ($\epsilon=4.9$)	Acetone ($\epsilon=20.7$)	Ethanol ($\epsilon=24.55$)	DMSO ($\epsilon=46.70$)	
Bond lengths (Å)							
N2-O3	1.214 (2)	1.227	1.230	1.231	1.231	1.231	1.227
N2-O4	1.219 (2)	1.226	1.230	1.231	1.231	1.231	1.225
N2-C11	1.465 (2)	1.470	1.462	1.459	1.459	1.459	1.473
N1-C8	1.407 (2)	1.392	1.394	1.396	1.396	1.396	1.394
N1-C7	1.308 (2)	1.340	1.336	1.334	1.333	1.333	1.290
C6-C7	1.403 (2)	1.387	1.392	1.394	1.395	1.395	1.445
C1-O1	1.298 (2)	1.254	1.263	1.268	1.268	1.269	1.339
O2-C9	1.346 (2)	1.360	1.355	1.354	1.354	1.354	1.360
N1-H11	0.960 (2)	1.041	1.037	1.035	1.035	1.035	-
O1-H11	-	-	-	-	-	-	0.991
Max dif. RMSE ^a		0.044 0.021					
Bond angles (°)							
O3-N2-O4	123.03 (12)	124.57	123.52	123.19	123.16	123.13	124.54
O3-N2-C11	118.12 (12)	117.65	118.20	118.38	118.40	118.41	117.69
O4-N2-C11	118.84 (12)	117.78	118.28	118.43	118.44	118.46	117.77
N2-C11-C10	117.99 (12)	118.67	118.68	118.66	118.65	118.66	118.51
C7-N1-C8	128.07 (10)	127.36	127.49	127.51	127.56	127.52	121.64
N1-C7-C6	122.79 (10)	123.33	123.37	123.40	123.35	123.37	122.35
O1-C1-C6-	121.43 (10)	121.62	121.60	121.59	121.59	121.57	122.25
O1-C1-C2	121.70 (10)	122.35	122.28	122.27	122.26	122.27	118.43
O2-C9-C8	116.98 (10)	115.93	116.07	116.25	116.27	116.26	117.06
C10-C9-O2	123.48 (11)	123.56	123.74	123.69	123.67	123.70	122.69
Max dif. RMSE ^a		1.06 0.827					
Torsion angles (°)							
C6-C7-N1-C8	179.82 (11)	-179.99	179.84	179.97	-179.99	179.93	176.51
C7-N1-C8-C9	-171.30 (11)	-179.99	179.39	179.72	179.69	179.81	-144.83
N1-C8-C9-C10	-178.38 (10)	-179.99	-179.97	-179.99	-179.97	-179.99	-178.16

^a Between the bond lengths and the bond angles computed by the theoretical method and those obtained from X-ray diffraction.

The experimental molecular structure, theoretical keto-amine counterpart and the enol-imine model of **I** are indicated in Figure 1 (a-b-c). The maximum deviation in keto-amine form geometry from the X-ray experimental geometry belongs to torsion angle C7-N1-C8-C9. The torsion angle C7-N1-C8-C9 is one of the angles controlling the planarity of molecule. Based on X-ray studies, the dihedral angle between the rings (C1-C6 and C8-C13) is 10.79(4)°, which shows that the conjugated part of the molecule is not planar. This angle has been calculated at 10.77 for gas-phase keto-amine form of **I** was calculated by using the same method. Schiff bases may display photochromic and thermochromic characteristics [4]. It is also known that molecules exhibiting photochromism are non-planar [14]. Thus, **I** shows a characteristic photochromism.

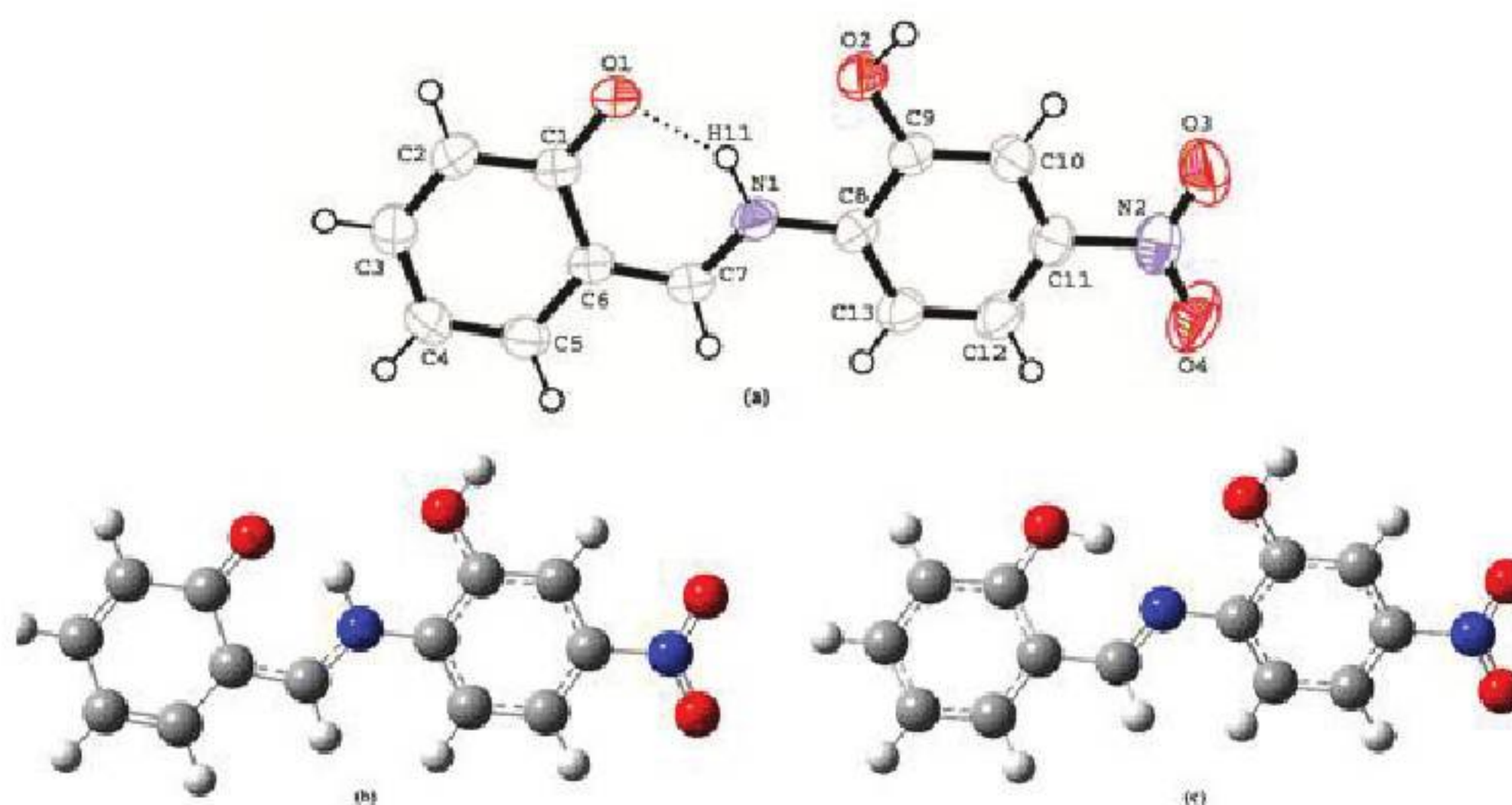


Figure 1. (a) Thermal ellipsoid plot of **I** [7]. (b) The theoretical geometric structures keto-amine form and (c) enol-imine form of **I**.

In order to compare the theoretical results with the experimental values for keto-amine form, root mean square error (RMSE) is used. Calculated RMSE for bond lengths and bond angles are 0.021 Å and 0.827° for B3LYP/6-311+G(d,p) method, respectively. A logical method for globally comparing the structure obtained with the theoretical calculation is by superimposing the molecular skeleton with that obtained from X-ray diffraction, giving a RMSE of 0.122 Å for B3LYP/6-311+G(d,p) (Figure 2). According to these results, it may be concluded that the B3LYP calculation well reproduce the geometry of **I**.

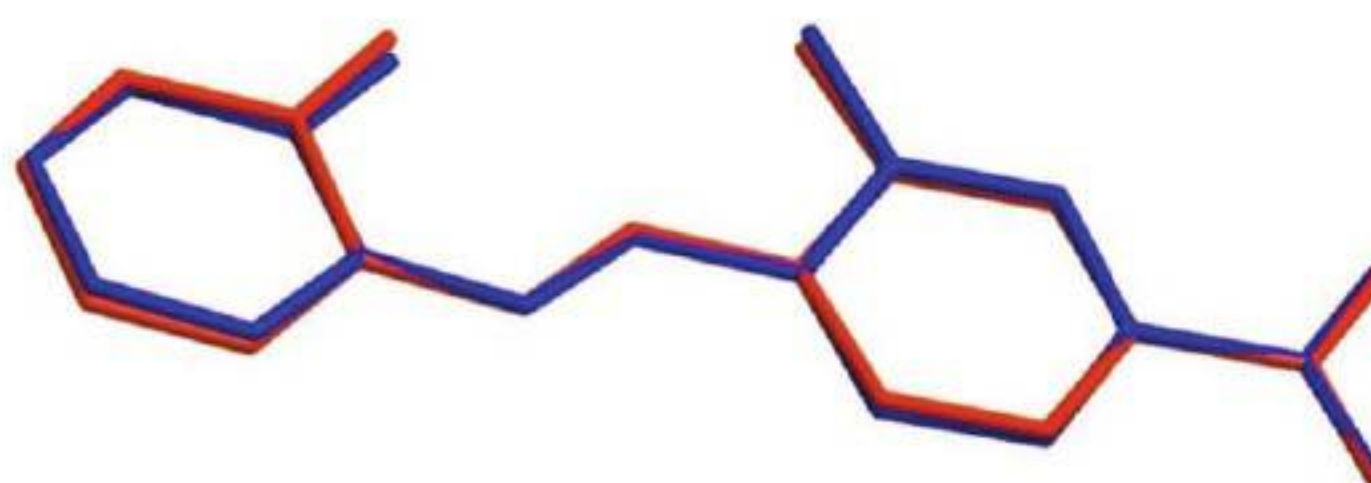


Figure 2. Atom-by-atom superimposition of the structures calculated (red) over the X-ray structure (blue) for **I**.

3.2. Total Energies in Gas-Phase and Solvent Media for Keto-Amine and Enol-Imine Tautomer Forms

In order to evaluate the energetic behavior of the compound in solvent media, we carried out calculations in gas-phase and four kinds of solvent (chloroform, acetone, ethanol, DMSO). The calculated total,

HOMO and LUMO energies, μ , η , χ and σ using the PCM by B3LYP/6-311+G(d,p) are collected in Table 2. According to Table 2, we can conclude that the total molecular energies and energy gap (ΔE), η of **I** obtained by PCM method decreases with the increasing polarity of the solvent, while the μ and σ will increase with the increase of the polarity of the solvent for keto-amine and enol-imine forms. Solvent effects improve the charge delocalized in the molecules, therefore, including the dipole moments to be raised. Ground-state dipole moment is an important factor in measuring solvent effect a large ground-state dipole moment gives rise to strong solvent polarity effects [15-16]. The β strongly related to the ΔE . In gas-phase, while the ΔE and LUMO is 2.7917 and η is 1.3959 eV for the keto-amine form of **I**, for the enol-imine form these values are 3.4382 and 1.7191 eV, respectively. The difference in the magnitudes of the η explains the difference between β values of the tautomers.

Table 2. Calculated energies, dipole moments (μ), global hardness (η) electronegativity (χ) and softness (σ) in gas-phase and solvent media for **I**.

DFT-B3LYP/6-311+G(d,p)					
Keto-amine form					
	Gas-Phase ($\epsilon=1$)	Chloroform ($\epsilon=4.9$)	Acetone ($\epsilon=20.7$)	Ethanol ($\epsilon=24.55$)	DMSO ($\epsilon=46.70$)
E_{total} (Hartree)	-911.95535	-911.9804509	-911.9901099	-911.9908127	-911.992079
E_{HOMO} (eV)	-6.0573	-5.9528	-5.9500	-5.9506	-5.9517
E_{LUMO} (eV)	-3.2656	-3.2545	-3.2678	-3.2684	-3.2711
ΔE (eV)	2.7917	2.6983	2.6822	2.6822	2.6806
η (eV)	1.3959	1.3492	1.3411	1.3411	1.3403
χ (eV)	4.6615	4.6037	4.6089	4.6095	4.6114
σ (eV) ⁻¹	0.7164	0.7412	0.7457	0.7457	0.7461
μ (D)	3.7574	4.5229	4.7848	4.8129	4.8482
Enol-imine form					
	Gas-Phase ($\epsilon=1$)	Chloroform ($\epsilon=4.9$)	Acetone ($\epsilon=20.7$)	Ethanol ($\epsilon=24.55$)	DMSO ($\epsilon=46.70$)
E_{total} (Hartree)	-911.96285	-911.9838418	-911.9917736	-911.9923015	-911.9933574
E_{HOMO} (eV)	-6.5373	-6.3977	-6.3715	-6.3715	-6.3675
E_{LUMO} (eV)	-3.0991	-3.1301	-3.1603	-3.1603	-3.1674
ΔE (eV)	3.4382	3.2676	3.2112	3.2112	3.2001
η (eV)	1.7191	1.6338	1.6056	1.6056	1.6001
χ (eV)	4.8182	4.7639	4.7659	4.7659	4.7675
σ (eV) ⁻¹	0.5817	0.6121	0.6228	0.6228	0.6250
μ (D)	4.6714	5.9266	6.3303	6.3586	6.4091

3.3. Prediction of First Hyperpolarizability – a NLO Property

Having the knowledge of NLO properties is of major importance in the design of materials in communication technology, signal processing, optical switches and optical memory devices [17]. The addition of donor and acceptor groups to conjugated systems also affects NLO properties in increasing way. The delocalization of π electron cloud on organic molecules increases in the case of powerful donor and acceptor groups. This is resulted in an increase in the α and β of organic molecules [18]. The μ , α , vector component along μ at zero frequency (β^{vec}) and β using the x, y, z components are defined as [19-20]:

$$\mu = \left(\mu_x^2 + \mu_y^2 + \mu_z^2 \right)^{1/2} \quad (1)$$

$$\alpha = (\alpha_{xx} + \alpha_{yy} + \alpha_{zz}) / 3 \quad (2)$$

[where α_{xx} , α_{yy} , and α_{zz} are the diagonal elements in the standard orientation of molecular polarizability tensor]

$$\beta^{\text{vec}} = \frac{3}{5} \left[\left(\beta_x^2 + \beta_y^2 + \beta_z^2 \right)^{1/2} \right] \quad (3)$$

$$\beta = \left(\beta_x^2 + \beta_y^2 + \beta_z^2 \right)^{1/2} \quad (4)$$

Here

$$\beta_x = \left(\beta_{xxx} + \beta_{xyy} + \beta_{xzz} \right) \quad (5)$$

$$\beta_y = \left(\beta_{yyy} + \beta_{xxy} + \beta_{yzz} \right) \quad (6)$$

$$\beta_z = \left(\beta_{zzz} + \beta_{xxz} + \beta_{yyz} \right) \quad (7)$$

The α and β are reported in atomic units (a.u.), the calculated values have been converted into electrostatic units (e.s.u.) (for α : 1a.u.= 0.1482×10^{-24} esu, for β : 1a.u.= 8.6393×10^{-33} esu). In order to investigate the NLO properties of **I**, the components of μ , α and the β were calculated using polar=ENONLY input to Gaussian 03 at the level of B3LYP/6-311+G(d,p) and the results obtained from calculation are given in Table 3.

Table 3. Calculated static dipole moment, linear polarizability, vector component along μ at zero frequency and the β components for **I**.

Components	B3LYP/6-311+G(d,p)	
	Keto-amine form	Enol-imine form
μ_i (D)		
μ_x	3.328	4.485
μ_y	-1.745	-0.897
μ_z	0.001	-0.950
μ_{tot}	3.758	4.671
α_{ij} (\AA^3)		
α_{xx}	65.331	56.736
α_{yy}	28.597	27.189
α_{zz}	13.500	15.193
α	35.809	33.039
$\beta_{ijk} \times 10^{-30}$ (cm^5/esu)		
β_{xxx}	-71.405	-48.091
β_{xxy}	-6.055	-4.427
β_{xyy}	2.714	1.596
β_{yyy}	-0.920	-2.114
β_{xxz}	0.001	-0.028
β_{yyz}	-0.001	-0.014
β_{xzz}	1.052	0.940
β_{yzz}	-0.597	-0.608
β_{zzz}	0.001	-0.187
β^{vec}	32.602	27.668
β	54.337	46.113

In our present work, the calculated μ , α , β^{vec} and β for **I** are 3.758 D, 35.809 \AA^3 , $32.602 \times 10^{-30} \text{ cm}^5/\text{esu}$, $54.337 \times 10^{-30} \text{ cm}^5/\text{esu}$ and 4.671 D, 33.039 \AA^3 , $27.668 \times 10^{-30} \text{ cm}^5/\text{esu}$, $46.113 \times 10^{-30} \text{ cm}^5/\text{esu}$ for keto-amine and enol-imine form, respectively. The highest value of the μ is found along μ_x . The direction of the μ_x values are 3.328 D for keto-amine form and 4.485 D for enol-imine form as shown in Table 3. In keto-amine and enol-imine forms; it was noticed that in β_{xxx} direction, which is the principal dipole moment axis, the smallest values of ten hyperpolarizability components as can be seen from Table 3 were noticed; and subsequently, electron cloud was more delocalized in the opposite of that direction.

3.4. NBO Analysis

The NBO analysis is a helpful tool for understanding of delocalization of electron density from occupied Lewis-type (donor) NBOs to properly unoccupied non-Lewis type (acceptor) NBOs within the molecule. The stabilization of orbital interaction is proportional directly to the energy difference between interacting orbitals. Therefore, the interactions having strongest stabilization take place between the effective donors and effective acceptors. The stabilization energy $E^{(2)}$ associated with i (donor) $\rightarrow j$ (acceptor) delocalization is estimated by the following equation [21]:

$$E^{(2)} = \Delta E_{ij} = -q_i \frac{F^2(i,j)}{\varepsilon_j - \varepsilon_i} \quad (8)$$

where q_i is the donor orbital occupancy, ε_i , ε_j are diagonal elements and $F(i,j)$ is the off-diagonal NBO Fock matrix element. In order to investigate the delocalization of electron density in the molecule B3LYP/6-311+G(d,p) method have been used for NBO analysis tautomeric form of **I**.

Selected second-order perturbation theory analysis of Fock matrix in NBO basis for **I** in gas-phase are listed in Table 4. Clearly seen from the table that the second-order perturbation theory analysis of Fock matrix in NBO basis shows strong intramolecular interactions for both tautomeric forms. These interactions are generally formed by orbital overlap between π (C-C) and π^* (C-C) orbitals in aromatic rings resulting in intramolecular charge transfer causing stabilization of the system. The NBO analysis of the tautomers have revealed some important interactions in the molecule. The lone pair of O3 donates its electrons to π -type antibonding orbital for N2-O4 with the stabilization energies of 671.291 kJ mol⁻¹ in keto-amine and 36.049 kJ mol⁻¹ in enol-imine form. These NBO interactions are pointed out the resonance effect in nitro group. In addition, the lone pair of O1 donates its electrons to the σ -type antibonding orbital N1-H11 resulting in stabilization of 72.894 kJ mol⁻¹. This interaction implies the existence of intramolecular hydrogen bond observed experimentally in keto-amine form. The experimental hydrogen bonding geometries are listed in Table 5. NBO analyses of the tautomeric forms confirm that the intramolecular charge transfer caused by π -electron cloud movement from donor to acceptor must be responsible for the NLO polarizability of **I**.

Table 4. Selected second-order perturbation theory analysis of Fock matrix in NBO basis for **I** in gas-phase.

Keto-amine form						
Bond type (<i>i</i>)	Donor (<i>i</i>)	Bond type (<i>j</i>)	Acceptor (<i>j</i>)	$E^{(2)a}$ (kJ mol ⁻¹)	$E(j)-E(i)^b$ (a.u.)	$F(i,j)^c$ (a.u.)
π	C2-C3	π^*	C1-O1	104.590	0.270	0.077
π	C4-C5	π^*	C2-C3	72.183	0.310	0.066
π	C6-C7	π^*	C1-O1	105.720	0.290	0.077
π	C6-C7	π^*	C4-C5	89.517	0.310	0.075
π	C8-N1	π^*	C6-C7	131.135	0.360	0.096
π	C9-C10	π^*	C8-N1	118.616	0.220	0.082
π	C12-C13	π^*	C8-N1	142.146	0.210	0.087
n2	O1	σ^*	C1-C2	67.661	0.780	0.102
n2	O1	σ^*	N1-H11	72.894	0.660	0.097
n2	O2	π^*	C9-C10	119.160	0.350	0.094
n2	O2	σ^*	O2-H21	78.882	2.160	0.186
n2	O3	σ^*	N2-O4	78.882	0.720	0.105
n3	O3	π^*	N2-O4	671.291	0.140	0.138
n2	O4	σ^*	N2-O3	79.677	0.720	0.106
Enol-imine form						
π	C1-C6	π^*	C4-C5	128.950	0.280	0.068
π	C1-C6	π^*	C7-N1	108.530	0.260	0.076
π	C2-C3	π^*	C1-C6	81.960	0.270	0.067
π	C2-C3	π^*	C4-C5	98.150	0.280	0.060
π	C4-C5	π^*	C1-C6	60.450	0.270	0.059
π	C4-C5	π^*	C2-C3	140.790	0.280	0.070
π	C7-N1	π^*	C8-C13	146.980	0.350	0.069
π	C8-C13	σ^*	C9-C10	63.720	0.280	0.067
π	C8-C13	σ^*	C11-C12	61.830	0.280	0.070
π	C9-C10	π^*	C8-C13	63.720	0.290	0.065
π	C9-C10	π^*	C11-C12	61.830	0.290	0.071
σ	C9-O2	σ^*	N2-O4	63.720	1.530	0.176
σ	C9-O2	π^*	N2-O4	61.830	3.400	0.740
π	C11-C12	π^*	C8-C13	54.850	0.290	0.066
π	C11-C12	π^*	C9-C10	54.850	0.280	0.067
n2	O1	π^*	C1-C6	78.150	0.320	0.104
n1	O2	π^*	N2-O4	55.010	3.090	0.368
n2	O2	π^*	C9-C10	78.400	0.340	0.095
n2	O2	σ^*	O2-H21	67.480	2.170	0.183
n2	O3	σ^*	N2-O4	48.450	0.900	0.108
n2	O3	σ^*	N2-O4	65.944	0.900	0.108
n3	O3	π^*	N2-O4	36.049	2.750	0.140
n2	O4	σ^*	N2-O3	48.450	0.730	0.109

^a $E^{(2)}$ means energy of hyper conjugative interactions.

^b Energy difference between donor and acceptor *i* and *j* NBO orbitals.

^c $F(i,j)$ is the Fock matrix element between *i* and *j* NBO orbitals.

Table 5. Feasible hydrogen bonds in **I** obtained from X-ray crystal data and B3LYP/6-311+G(d,p) method.

D-H...A	D-H (Å)	H...A (Å)	D...A (Å)	D-H...A (°)
N1-H11...O1	(0.960)	(1.76)	(2.579)	(142.0)
N1-H11...O1 (keto-amine form)	1.041	1.741	2.602	137.2
O1-H11...N1 (enol-imine form)	0.991	1.762	2.641	145.7

The experimental values are given in parenthesis.

3.5. FMOs

The HOMO and LUMO of **I** are shown in Figure 3. The frontier orbital of a chemical species are very important in defining its reactivity. The green and red colours represent the negative and positive values for the wave function. The HOMO is the orbital that primarily acts as an electron donor and the LUMO is the orbital that mainly acts as an electron acceptor [18]. In our investigation we found that our title compound has a total of 476a alpha orbitals out of which 1a-67a are occupied alpha orbitals while 68a-476a are virtual orbitals. Out of these 476a alpha orbitals the orbital numbered as 67a is HOMO orbital and 68a is LUMO orbital. As seen in Figure 3, in the HOMO for keto-amine form and enol-imine form, the charge density are mainly delocalized over the molecule except N2 atom. However, in case of the LUMOs are mainly delocalized over the molecule, except O2 atom for keto-amine form and except O2, C4 and C6 atom for enol-imine form, respectively.

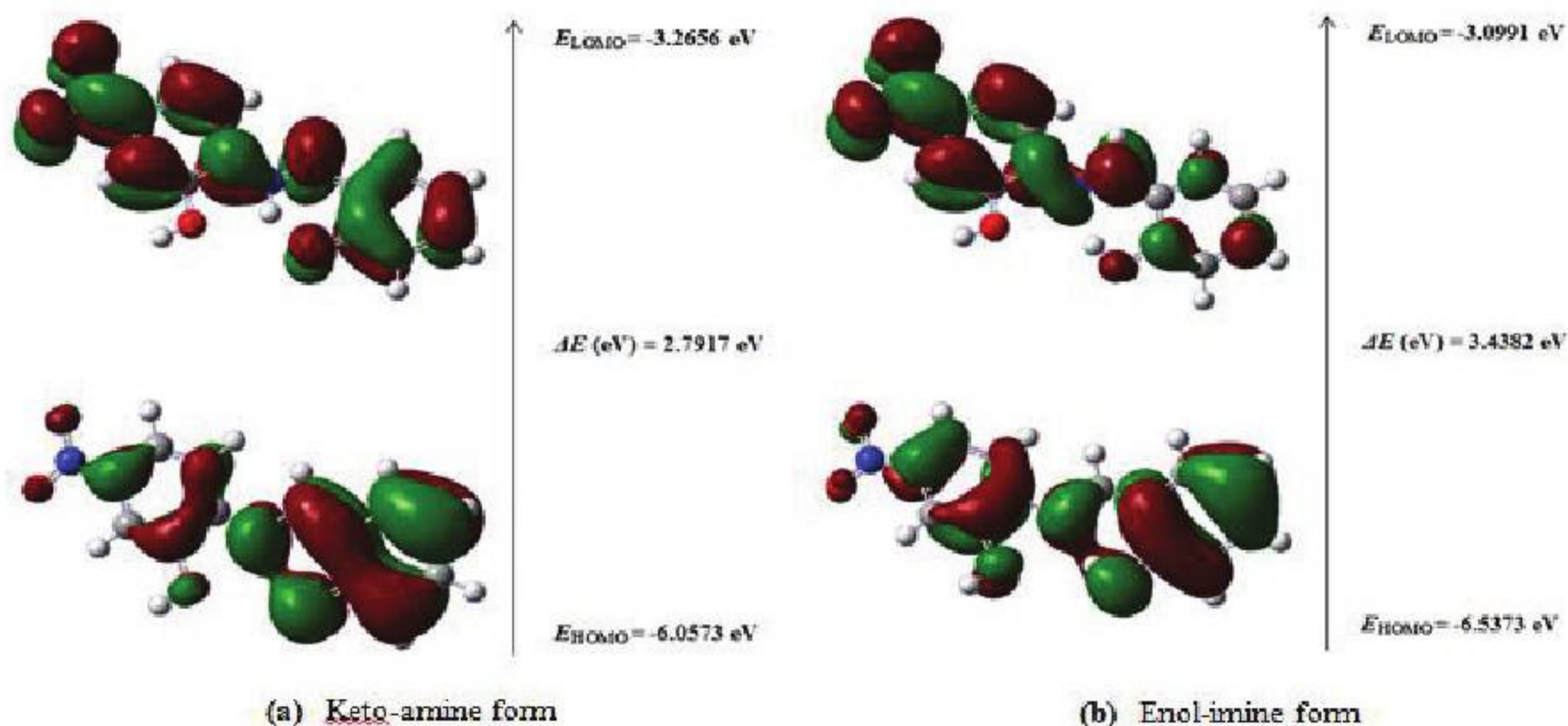


Figure 3. HOMO and LUMO energy levels for **I**.

3.6. MEP

The MEP is used primarily for predicting sites and relative reactivity towards electrophilic and nucleophilic attacks, and in predicting the hydrogen bonding interactions [22]. The MEP of the **I** calculated using the optimized geometry at the B3LYP/6-311+G(d,p) basis set is used to predict the reactive sites for electrophilic and nucleophilic attack. As shown Figure 4, yellow and red colors indicated for the negative regions of the MEP are related to electrophilic reactivity, while blue colors indicated for positive regions to nucleophilic reactivity. As shown in, **I** has three possible site for electrophilic attack. The oxygen atoms (O1, O3 and O4) have negative region. The negative molecular electrostatic potential values are -0.051, -0.044 and -0.039 a.u. for the mainly region of the O1, O3 and O4 atoms, respectively. The O2-H2O and C7-H7 bonds indicating possible site for nucleophilic attack with maximum values of 0.077 and 0.045 a.u. around of these bonds have maximum positive regions, respectively. Based on these calculated results, the region of MEP shows that the most negative region is localized on atom O1 which will be the preferred site for electrophilic attack. However, the most preferred region for and nucleophilic attack will be on H2O.

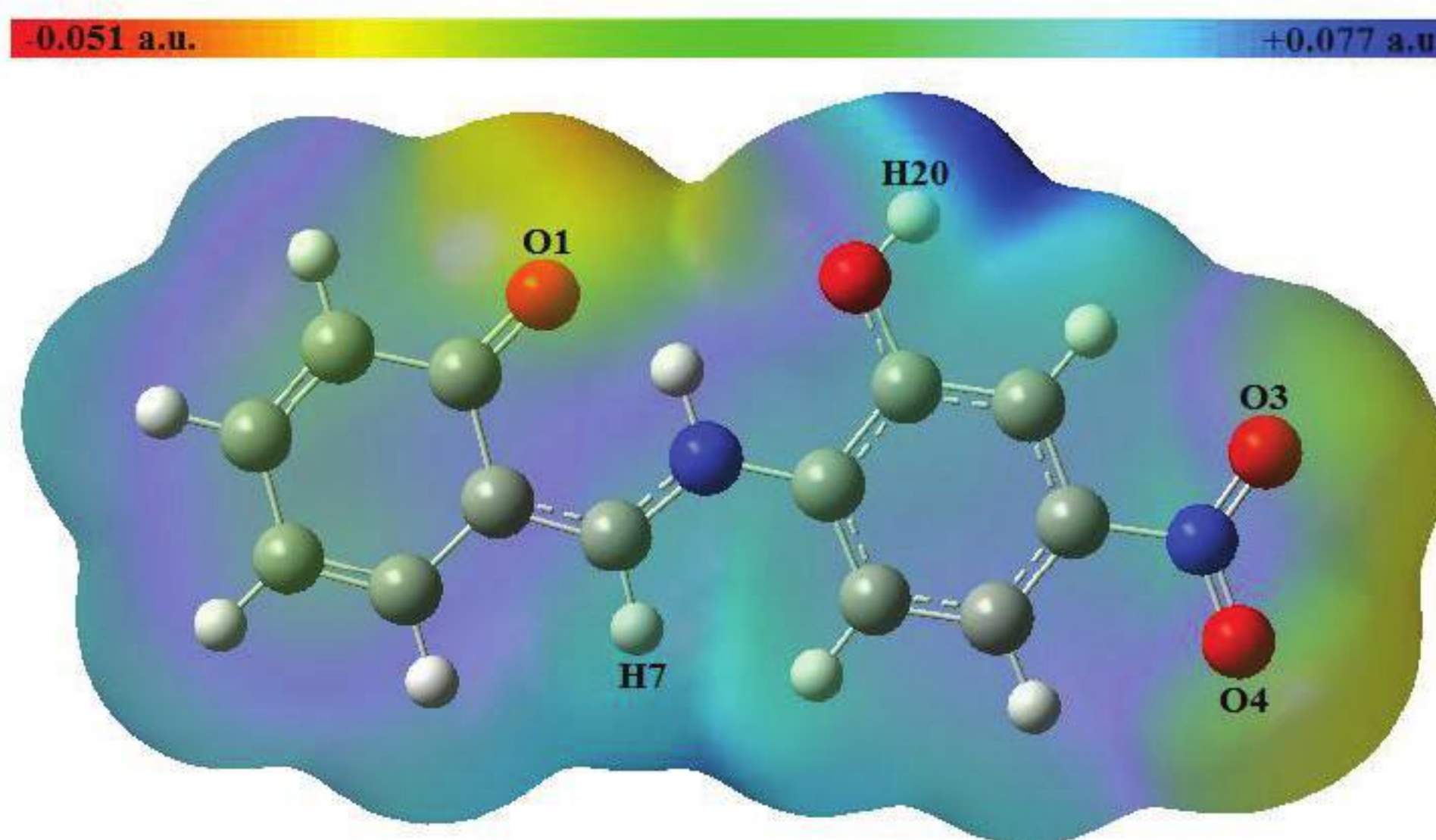


Figure 4. MEP maps of **I** calculated at B3LYP/6-311+G(d,p) level.

3.7. Thermodynamic Properties

The values of thermodynamic parameters such as specific heat capacity ($C_{p,m}^0$), entropy (S_m^0), and enthalpy (H_m^0) of **I** by B3LYP/6-311+G(d,p) basis set was calculated and listed in Table 6.

Table 6. Thermodynamic properties at different temperatures at the B3LYP with basis set 6-311+G(d,p) level for **I**.

Molecule	Temperature (K)	$C_{p,m}^0$ (cal/mol-K)	S_m^0 (cal/mol-K)	H_m^0 (kcal/mol)
Keto-amine form	100	24.130	86.245	1.543
	150	33.021	98.500	2.970
	200	42.333	109.839	4.852
	250	51.820	120.747	7.206
	298.15	60.820	130.998	9.919
	300	61.159	131.388	10.032
Enol-imine form	100	23.494	84.360	1.496
	150	32.329	96.341	2.889
	200	41.674	107.484	4.737
	250	51.228	118.253	7.060
	298.15	60.307	128.406	9.746
	300	60.649	128.792	9.858

As observed from Table 6, values of heat capacity, entropy and enthalpy increase of temperature from 100 to 300 K which is attributed to the enhancement of the molecular vibration while the temperature increases. The relation among energetic, structural and reactivity characteristics of the molecule may be obtained from the thermodynamic parameters of the compounds. The observed relations of the thermodynamic functions vs. temperature with the regression factors not less than 0.9999 for the keto-amine and enol-imine form in **I** are given by:

Keto-amine form

$$\begin{aligned}
 C_{p,m}^0(T) &= 6.3916 + 0.1739T + 1.0502 \times 10^{-5} T^2, \quad R^2 = 0.99995 \\
 S_m^0(T) &= 60.7051 + 0.2664T - 1.0314 \times 10^{-5} T^2, \quad R^2 = 0.99995 \\
 H_m^0(T) &= 0.1038 + 0.0051T + 9.3376 \times 10^{-5} T^2, \quad R^2 = 1
 \end{aligned}
 \tag{9}$$

Enol-imine form

$$\begin{aligned}
 C_{p,m}^0(T) &= 5.9393 + 0.1711T + 3.8082 \times 10^{-5} T^2, \quad R^2 = 0.99994 \\
 S_m^0(T) &= 59.5095 + 0.2584T - 9.1756 \times 10^{-5} T^2, \quad R^2 = 0.99996 \\
 H_m^0(T) &= 0.1360 + 0.0042T + 9.3899 \times 10^{-5} T^2, \quad R^2 = 1
 \end{aligned}
 \tag{10}$$

The correlation graphs are shown in Figure 5. All these thermodynamic data provide helpful information for the further studies on **I**. They can be used to compute the other thermodynamic parameters according to relationships of thermodynamic functions and to determine the directions of chemical reactions according to the second law of thermodynamics.

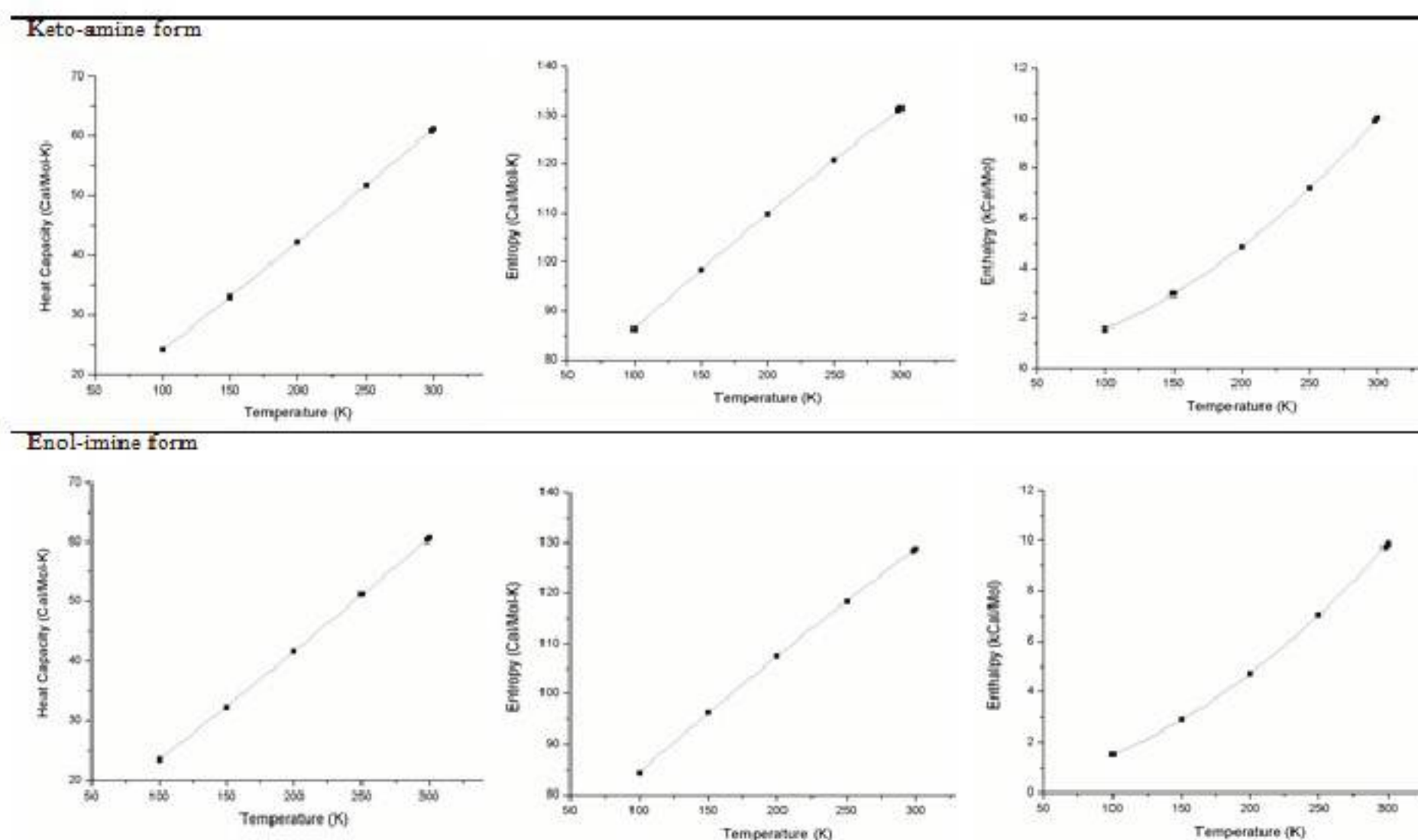


Figure 5. Correlation graphics of thermodynamic properties and temperatures for **I**.

3.8. Mulliken Population Analysis

The Mulliken atomic charges affect dipole moment, α , electronic structure and more a lot of properties of molecular systems. The total atomic charges of **I** in gas-phase for keto-amine form are obtained by Mulliken population analysis with B3LYP/6-31G(d) method and are listed in Table 7. Illustration of atomic charges plotted is shown in Figure 6. As seen in Table 7 and Figure 6, all the hydrogen atoms have net positive charges within range from 0.1281 to 0.4342 in the gas-phase. The H11 atom has bigger positive atomic charge than the other hydrogen atoms. This is due to the N-H...O interaction. As expected, the results show that the charge of the nitrogen atom N1 in imine group is negative, but the charge of the nitrogen atom bonded to C8-C13 ring, the charge of N2, is positive. There is a large accumulation of positive charge on atom N2 and negative charge on O3 in **I**. Therefore, this might had given (N2-O3) bond a greater ionic character.

Table 7. Mullikan charge distribution of **I** in gas-phase for keto-amine form using B3LYP/ 6-31G(d) method.

Atom	Charge
C1	0.4106
C2	-0.1796
H2	0.1398
C3	-0.1161
H3	0.1380
C4	-0.1581
H4	0.1320
C5	-0.1672
H5	0.1281
C6	0.0369
C7	0.0743
H7	0.1719
C8	0.3801
C9	0.3148
C10	-0.2340
H10	0.1793
C11	0.2803
C12	-0.1707
H12	0.1840
C13	-0.1842
H13	0.1547
N1	-0.7249
N2	0.3805
O1	-0.5919
O2	-0.6403
O3	-0.4018
O4	-0.3980
H11	0.4342
H21	0.4273

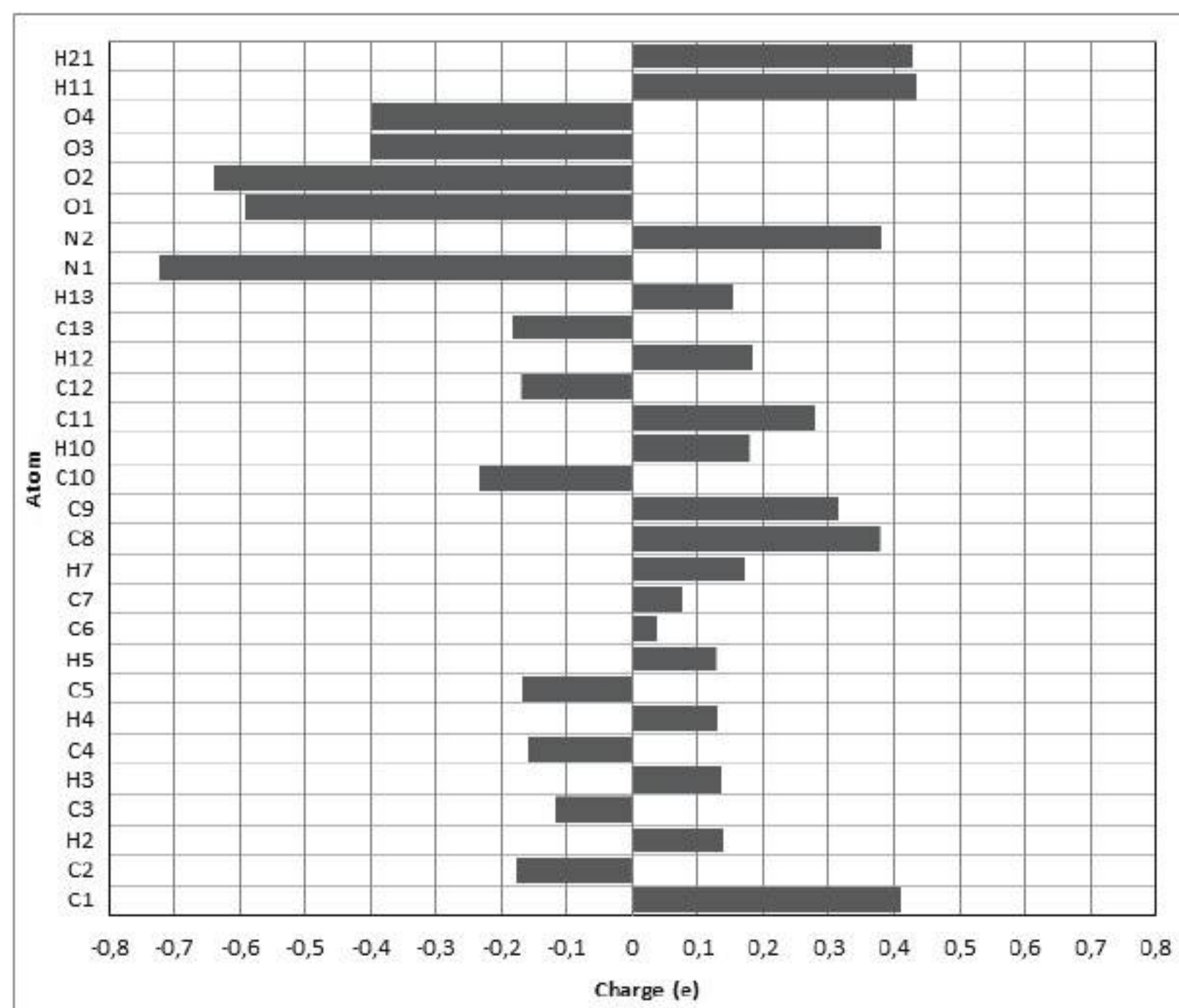


Figure 6. Illustration of atomic charges plotted of **I** in gas-phase for keto-amine form using DFT-B3LYP/6-31G(d).

At the same time, the Mulliken atomic charges for the non-H atoms of **I** were calculated at B3LYP/6-31G(d) level in gas-phase. In order to investigate the solvent effect selected three kinds of solvent, the atomic charge distributions of **I** were also calculated at B3LYP/6-31G(d) level. The calculated values of atomic charges of **I** in gas-phase and solution-phase listed as shown in Table 8. According to the calculated Mulliken atomic charges, the N1 and O1 atoms have bigger negative atomic charges in gas-phase. But then, as shown in Table 8, the atomic charge values of the N1 and O1 atoms in solution-phase are bigger than those in gas-phase and while their atomic charges are becoming more negative with the increase of the polarity of the solvent.

Table 8. The calculated Mullikan charges for the non-H atoms of **I** in gas-phase and solution-phase for keto-amine form using B3LYP/6-31G(d) method.

Atom	Gas-Phase ($\epsilon = 1$)	Solution-Phase		
		Chloroform ($\epsilon=4.9$)	Ethanol ($\epsilon=24.55$)	Water ($\epsilon=78.39$)
C1	0.040976	0.017710	0.016994	0.016667
C2	-0.039468	-0.053421	-0.060562	-0.064009
C3	0.021491	0.032573	0.032554	0.032491
C4	-0.025549	-0.025650	-0.026191	-0.026522
C5	-0.041153	-0.018457	-0.015000	-0.014037
C6	0.407934	0.405339	0.398869	0.396497
C7	0.248462	0.275565	0.301149	0.309765
C8	0.372204	0.377647	0.371875	0.366937
C9	0.323739	0.316376	0.317544	0.323664
C10	-0.053061	-0.035417	-0.029835	-0.027438
C11	0.288821	0.283248	0.295183	0.299270
C12	0.016573	0.014984	0.016388	0.017011
C13	-0.025660	-0.008458	0.002469	0.008901
N1	-0.285594	-0.295880	-0.296188	-0.296636
N2	0.362019	0.379353	0.380709	0.375629
O1	-0.598893	-0.604905	-0.646722	-0.658275
O2	-0.213124	-0.204031	-0.189996	-0.187870
O3	-0.401526	-0.426128	-0.434667	-0.437249
O4	-0.398189	-0.426449	-0.434575	-0.437796

4. CONCLUSION

In the present work, the density functional calculations on **I** beginning from the X-ray data have been performed. The objectives of this study to reproduce the molecular geometry, energy gap, non-linear optical and thermodynamic properties of **I** for the further studies. The geometric parameters, and electronic and optical properties of **I** was calculated at the B3LYP/6-311+G(d,p) level. Atomic charges on the various atoms of **I** obtained by Mulliken's population analysis. It was also observed that there is a large accumulation of positive charge on atom N2 and negative charge on O3 in **I** molecule. Therefore, this might had given (N2-O3) bond a greater ionic character. The first calculated hyperpolarizabilities using B3LYP/6-311+G(d,p) level for keto-amine and enol-imine form were found $32.602 \times 10^{-30} \text{ cm}^5/\text{esu}$ and $46.113 \times 10^{-30} \text{ cm}^5/\text{esu}$, respectively. To predict reactive sites for electrophilic and nucleophilic attack for the investigated molecule, MEP studies were carried out. Thus, it would be predicted that the oxygen atom will be the most reactive site for electrophilic attack and hydrogen atom will be the reactive site for nucleophilic attack. Also, the NBO analysis and FMOs constitute maximal absorption confirm that the intramolecular charge transfer caused by π -electron cloud movement must be responsible for the NLO properties of the tautomers. Keto-amine and enol-imine forms of compound are good candidates for NLO materials due to the magnitudes of their β . As a result, this work will help to design and synthesis new materials.

REFERENCES

- [1] M. D. Cohen, G. M. J. Schmidt, and S. Flavian, "Experiments on photochromy and thermochromy of crystalline anils of salicylaldehydes", *J. Chem. Soc.*, 2041-2051 (1964).
- [2] H. S. Maslen, and T. N. Waters, "The conformation of Schiff-base complexes of copper(II)", *Coord. Chem. Rev.*, 17, 137-176 (1975).
- [3] J. M. Stewart, and E. C. Lingafelter, "The crystal structure of bis-salicylaldiminato-nickel(II) and -copper(II)", *Acta Cryst.*, 12, 842-845 (1959).
- [4] E. Hadjoudis, M. Vitterakis, and I. Moustakali-Mavridis, "Photochromism and thermochromism of schiff bases in the solid state and in rigid glasses", *Tetrahedron*, 43, 1345-1360 (1987).
- [5] I. Moustakali-Mavridis, E. Hadjoudis, and A. Mavridis, "Crystal and Molecular Structure of Thermochromic Schiff Bases II. Structures of N-salicylidene-3-aminopyridine and N-(5-methoxy-salicylidene)-3-aminopyridine", *Acta Cryst.*, B36, 1126-1130 (1980).
- [6] P. M. W. Gill, B. G. Johnson, J. A. Pople, and M. J. Frisch, "The performance of the Becke-Lee-Yang-Parr (BLYP) density functional theory with various basis sets", *Chem. Phys. Lett.*, 197, 499-505 (1992).
- [7] C. C. Ersanli, Ç. Albayrak, M. Odabaşoğlu, and A. Erdönmez, "2-[(2-Hydroxy-4-nitrophenyl)aminomethylene]-cyclohexa-3,5-dien-1(2H)-one", *Acta Cryst.*, C59, 601-602 (2003).
- [8] A. D. Becke, "Density-functional thermochemistry. III. The role of exact exchange", *J. Chem. Phys.*, 98, 5648-5652 (1993).
- [9] M. J. Frisch et al., *Gaussian 03*, Gaussian, Inc., Wallingford, CT, (2004).
- [10] R. Dennington II, T. Keith, and J. Milliam, *GaussView*, Version 4.1.2. Semichem Inc., Shawnee Mission, KS, (2007).
- [11] S. Miertus, E. Scrocco, and J. Tomasi, "Electrostatic interaction of a solute with a continuum. A direct utilization of AB initio molecular potentials for the prevision of solvent effects", *J. Chem. Phys.*, 55, 117-129 (1981).
- [12] V. Barone and M. Cossi, *J. Phys. Chem. A* 102, 1995-2001 (1998).
- [13] E. D. Glendening, A. E. Reed, J. E. Carpenter, and F. Weinhold, *NBO Version 3.1*, CI, University of Wisconsin, Madison, 2003.
- [14] I. Moustakali-Mavridis, E. Hadjoudis, and A. Mavridis, "Crystal and Molecular Structure of Some Thermochromic Schiff Bases", *Acta Cryst.*, B34, 3709-3715 (1978).
- [15] A. Masternak, G. Wenska, J. Milecki, B. Skalski, and S. Franzen, "Solvatochromism of a Novel Betaine Dye Derived from Purine", *J. Phys. Chem. A* 109, 759-766, (2005).
- [16] Y. Le and J.F. Chen, M. Pu, "Electronic structure and UV spectrum of fenofibrate in solutions", *Int. J. Pharm. Sci.*, 358, 214-218 (2008).
- [17] S. L. Guo, T. P. Li, T. B. Wang, Z. S. Liu, and T. D. Cao, "Third-order nonlinearities and optical limiting properties of complex Co2L3", *Opt. Mater.*, 29, 494-498 (2007).
- [18] K. S. Thanthiriwatte, and K. M. Nalin de Silva, "Non-linear optical properties of novel fluorenyl derivatives-ab initio quantum chemical calculations", *J. Mol. Struct.*, 617, 169-175 (2002).
- [19] Y. X. Sun, Q. L. Hao, Z. X. Yu, W. X. Wei, L. D. Lu, and X. Wang, "Experimental and density functional studies on 4-(4-cyanobenzylideneamino)antipyrine", *Mol. Phys.*, 107, 223-235 (2009).
- [20] R. Zhang, B. Du, G. Sun, and Y. Sun, "Experimental and theoretical studies on o-, m- and p-chlorobenzylideneaminoantipyrines", *Spectrochim. Acta A* 75, 1115-1124 (2010).
- [21] F. Weinhold, and C. R. Landis, "Natural bond orbitals and extensions of localized bonding concepts", *Chem Educ. Res. Pract. Eur.*, 2, 91-104 (2001).

[22] J. S. Murray, and K. Şen, Molecular Electrostatic Potentials, Concepts and Applications, Elsevier, Amsterdam, (1996).